# Exploring Cheminformatic Toolsets for Predicting the Dermal Toxicity of Furanocoumarins

**Douglas Vieira Thomaz** [1], **Matheus Gabriel de Oliveira** [1], **Vinicius Barreto da Silva** [2], **Pierre Alexandre dos Santos** [1], **Rene Oliveira do Couto** [3]

[1] *Universidade Federal de Goiás*
240 street, Leste Universitário district, Goiânia - GO, 74605-170, Brazil

[2] *Pontifical Catholic University of Goiás*
1,440 street, University, Setor Universitário, Goiânia - GO, 74605-010, Brazil

[3] *Universidade Federal de São João del-Rei*
Campus Centro-Oeste Dona Lindu. Sebastião Gonçalves Coelho St., n. 400, Divinópolis, MG, 35501-296, Brazil

DOI: 10.22178/pos.74-6

LCC Subject Category: RM1-950

Received 21.08.2021
Accepted 25.09.2021
Published online 30.09.2021

Corresponding Author:
Rene Oliveira do Couto
rocouto@ufsj.edu.br



**Abstract.** Linear furanocoumarins are skin sensitizers and anticancer agents whose appeal in skincare therapeutics is widely exploited. Owing to the need to predict the biological activities of medicines, this work aimed the investigate the predicted dermal toxicity of linear furanocoumarins through chemoinformatic approaches**.** Therefore, eight major linear furanocoumarins of interest in medicine were selected, and their pharmacophores / toxicophores were modelled and inputted in several databases and cheminformatic toolsets previously described in the literature. Moreover, Principal Components Analysis was performed to allow multivariable comparisons. Results showcased that the first two PCs accounted for 95.48% of all variance in the model, and molecular weight and polar surface showcased a positive correlation to Log P and Log $K_p$, which may be involved in skin penetration. Moreover, the pharmacophore modelling evidenced superimposition between linear furanocoumarins, ethidium bromide and acridine orange, thereby suggesting that these compounds share similar biological effects, supported by their acknowledged DNA intercalating activities. Therefore, this work showcased the application of various cheminformatic tools to screen the dermal toxicity of chemicals.

**Keywords:** skin sensitizer; DNA intercalation; secondary metabolite; *in silico*; molecular modelling.

## INTRODUCTION

Linear furanocoumarins (LF) or psoralens are secondary plant metabolites whose appeal in therapeutics is widely exploited in folk and standard medicine practices [1, 2, 3]. These compounds are biosynthesized from intermediaries of polyketide and mevalonate pathways, and their chemical structures showcase high variability, being only ever-present the core-moiety furo [3, 2-g] chromen-7-one. Although psoralens may vary in sidechain composition and conformation, these compounds do exhibit similar physicochemical features due to the substantial electron donor and accepting properties of their central aromatic system, which not only provides them similar electroactivity to several aromatic natural and synthetic compounds [4–10] but also confers photoreactivity to them upon the incidence of radiation at ≈ 340–365 nm (*i.e.* near the end of the ultraviolet spectrum) [1].

Considering the biological activities of LF, the furo [3, 2-g] chromen-7-one core-moiety is acknowledged to bind covalently to some therapeutic targets such as DNA bases [11–13]. This process is regarded as one of the main underlying factors regarding these compounds' therapeutic and toxic effects [3]. Notwithstanding, several authors reported that psoralens interact with many macromolecules in the human organism, which may be involved in their medicinal uses against cancer, psoriasis, vitiligo and other health conditions [2, 14, 15].

According to standard healthcare protocols, LF use in therapeutics is conditioned by either enteral or parenteral administration, being the drug uptake route decided according to the diagnosis

and overall state of the patient [1]. In general terms, LF therapeutics rely on controlled patient exposure to ultraviolet radiation, given the dependence of the clinical outcome to this approach [2]. The patient exposure to ultraviolet light is supported by several authors, who described the remarkable effects of radiation on the thermodynamic feasibility of psoralens binding to DNA and other biomolecules, suggesting that photoactivation is involved in the pharmacodynamics of these compounds [2, 13]. Furthermore, some authors reported the benefits of *in situ* skin administration of LF-containing formulations and ultraviolet exposure to directly treat an affected area [1, 16, 17].

Although LF topical use in medicine is well reported, the extent of their dermal toxicity is still an issue [18, 19]. Despite not being considered outright toxic, these compounds are highly photoreactive, and the still unknown consequences of their phototoxicity upon the incidence of ultraviolet radiation daily is a significant concern to long term treatments [14]. In this sense, the comprehensive investigation of the dermal effects of LF is of particular importance to promote patient safety and ensure treatment efficacy.

Several in vitro and in vivo assays are commonly used to assess if new formulations are adequate to patient safety standards regarding dermal drug toxicity. Amongst these assays are murine local lymph node assay (LLNA) [20], direct peptide reactivity assay (DPRA) [21], human cell-line activation test (H-CLAT) [22] and KeratinoSens® [23], which provide essential information regarding skin sensitization and dermal toxicity. Albeit reliable and effective in providing information on possible toxic effects and their mechanisms, some of these tests are expensive and require adequate infrastructure to perform [24]. Moreover, most *in vitro* approaches are time and reagent consuming, hindering their application for large output products such as toxicological screenings. In this sense, alternative methods such as cheminformatic investigations could provide complementary information regarding the dermal toxicity of compounds bearing similar chemical structures, such as LF.

Cheminformatic is a relatively new field of research and involves using computational resources to investigate chemical phenomena. This approach uses the physicochemical features of compounds converted to usable data through mono or multidimensional molecular descriptors [25–28]. This information can be correlated to databases or using data mining and machine learning algorithms to establish predictive models regarding biological activity, pharmacophores [30], docking models [27, 28, 31, 32], and other applications. Notwithstanding, these studies can be performed on free software, *i.e.*, freeware, for most scientific applications. This further increases their appeal as low-cost alternatives to primarily investigate drug biological activities or complementary techniques to guide *in vitro* and *in vivo* assays.

Therefore, because of the therapeutic relevance of LF for skin conditions, and the importance of inciting information regarding their toxicity upon topical use, this work investigates the predicted dermal toxicity of LF thence through chemoinformatic approaches. Henceforth several databases and toolsets previously described in the literature were used, and their results were compared.

## MATERIALS AND METHODS

*LF chemical structures***.** In this study, 8 LF were selected, namely: bergamottin (BTI), bergapten (BTN), bergaptol (BTO), imperatorin (IMP), isopimpinellin (ISO), psoralen (PSO), trioxalen (TRI) and xanthotoxin (XTN). Moreover, two known DNA intercalating agents were also selected to allow comparisons to be drawn from the pharmacophore modelling, being them acridine orange and ethidium bromide.

*Study design and data pre-treatment***.** This work focused initially to gather information regarding the physicochemical and biological properties of the selected LF. Therefore, Pubchem database was used to retrieve isomeric (when available) or canonical simplified molecular-input line-entry system (SMILES) of each compound [33]. This information was used without further treatment in Molinspiration [34], pkCSM [35], SwissADME [36, 37] and Pred-Skin [38, 39] cheminformatic tools.

Thereafter, the SMILES string of each compound was converted to a three-dimensional rendering of their chemical structures whereupon charges were assigned using Biovia Discovery Studio® software. Manual corrections regarding aromatic bonds were also conducted, and all structures were thoroughly reviewed before further experiments.

All treated structures were added to a single file and submitted to PharmaGist Webserver [40, 41]. The work conditions were: 5 output pharmacophores, PSO as key-molecule and a minimum of 3 features in the predicted model. Furthermore, we employed the following feature weightings in the proposed models: 3.0 for aromatic rings, 1.0 for charge (anion/cation), 1.5 for hydrogen bond (donor/acceptor), 0.3 for hydrophobic. The higher weighting for aromatic rings was selected considering the particularities of LF, given the abundance of π-electrons in their common core-moiety, namely furo [3, 2-g] chromen-7-one.

All figures were rendered and treated using Biovia Discovery Studio® software.

*Statistical analysis.* To investigate any possible trend in the physicochemical data of the compounds, Principal Component Analysis (PCA) was used [42]. This approach was selected to minimize dataset dimensions basing on variance/correlation matrix. Statistical significance was attributed to $p < 0.05$. All statistical analysis was performed using Origin Pro 9b® software package (Northampton, MA, USA).

## RESULTS AND DISCUSSION

The first step of this investigation involved the assessment of the predicted physicochemical properties of each compound. Therefore, pkCSM and Molinspiration databases were used. All information above is showcased in Table 1.

Table 1 – Predicted physicochemical properties of linear furanocoumarin derivatives, namely: BTI, BTN, BTO, IMP, ISO, PSO, TRI and XTN*

| | MW** | Log P | Rb** | Hb** acceptor | Hb** donor | SA** | PSA** | LipinskiV** |
|---|---|---|---|---|---|---|---|---|
| BTI | 338.403 | 5.6107 | 6 | 4 | 0 | 145.939 | 52.59 | 1 |
| BTN | 216.192 | 2.5478 | 1 | 4 | 0 | 90.034 | 52.59 | 0 |
| BTO | 202.165 | 2.2448 | 0 | 4 | 1 | 83.350 | 63.58 | 0 |
| IMP | 270.284 | 3.8842 | 3 | 4 | 0 | 114.804 | 52.59 | 0 |
| ISO | 246.218 | 2.5564 | 2 | 5 | 0 | 101.512 | 61.82 | 0 |
| PSO | 186.166 | 2.5392 | 0 | 3 | 0 | 78.555 | 43.35 | 0 |
| TRI | 228.247 | 3.4644 | 0 | 3 | 0 | 97.650 | 43.35 | 0 |
| XTN | 216.192 | 2.5478 | 1 | 4 | 0 | 90.034 | 52.59 | 0 |

Notes: *All data gathered at pkCSM and Molinspiration databases upon imputing the SMILES string of each compound.
**Calculated molecular properties at pkCSM. MW - molecular weight; Rb – rotatable bonds; Hb – hydrogen bond; SA – surface area.
*** Calculated properties at Molinspiration. PSA – polar surface area; LipinskiV – Lipinski rules violations.

Results showcased that all compounds ranged from 186.166 to 338.403 g mol-1 and their Log P ranged from 2.2448 to 5.6107. BTI showcased the highest amount of rotatable bonds, *i.e.,* 6, while BTO, PSO and TRI showcased none. Regarding hydrogen bond formation, most molecules showcased four acceptors and no donors. Concerning surface and polar surface areas, all compounds ranged from 78.555 to 145.939 and from 43.35 to 63.58, respectively. Furthermore, a single Lipinski rule violation was detected for BTI (Table 1).

To investigate the pharmacokinetic properties of LF upon non-invasive cutaneous administration, their predicted skin permeability profiles were assessed by gathering data regarding Log $K_p$ from different databases. Moreover, other predictive pharmacokinetic information was also gathered, namely: blood-brain barrier permeability (Log BB), one-way flux level corrected with the brain flux value representing the central nervous system permeability (Log PS), and intestinal permeability (IA). Results are showcased in Table 2.

Results show that predicted Log $K_p$ values differ according to the consulted source, though expressed in different dimensions. For example, log $K_p$ from source A (pkCSM) ranged from -2.216 to -2.830 cm h, while from source B (SwissADME), the values ranged from -4.61 to -6.40 cm s. Log BB and log PS, which correlate to the distribution of the drugs through cerebrospinal fluid, ranged from 0.085 to 0.447 and from -1.639 to -2.834, respectively. Furthermore, predicted intestinal absorption for all drugs was above 95%, the highest recorded of 98.386% for ISO (Table 2).

Table 2 – Predicted pharmacokinetic properties of linear furanocoumarin derivatives, namely: BTI, BTN, BTO, IMP, ISO, PSO, TRI and XTN*

| | Log $K_p$ A** | Log $K_p$ B*** | Log BB** | Log PS** | IA** |
|---|---|---|---|---|---|
| BTI | - 2.520 | - 4.61 | 0.085 | - 1.840 | 95.727 |
| BTN | - 2.419 | - 6.25 | 0.202 | - 2.830 | 98.344 |
| BTO | - 2.830 | - 6.40 | 0.380 | - 2.803 | 93.911 |
| IMP | - 2.351 | - 5.46 | 0.176 | - 1.905 | 97.755 |
| ISO | - 2.440 | - 6.40 | 0.123 | - 2.834 | 98.386 |
| PSO | - 2.216 | - 6.25 | 0.410 | - 1.714 | 96.668 |
| TRI | - 2.223 | - 5.46 | 0.447 | - 1.639 | 97.372 |
| XTN | -2.336 | - 6.20 | 0.245 | - 2.028 | 98.341 |

Notes: *All data gathered at pkCSM and SwissADME databases upon imputing the SMILES string of each compound.

**Calculated properties at pkCSM. Log $K_p$ A – skin permeability (cm h); Log BB – blood-brain barrier permeability; Log PS – constant of one-way flux level corrected with the brain flux value representing the central nervous system permeability; IA – intestinal absorption (%).

***Calculated properties at SwissADME. Log $K_p$ B – skin permeation (cm s).

After gathering data regarding each compound's predicted physicochemical and pharmacokinetic features, molecular weight, Log P, surface and polar surface areas were investigated as independent and continuous variables through PCA analysis. This was performed to analyze if the reported values showcased any LF skin absorption behaviour trend, which Log Kp represents. Results are showcased as PCA biplot in Figure 1.

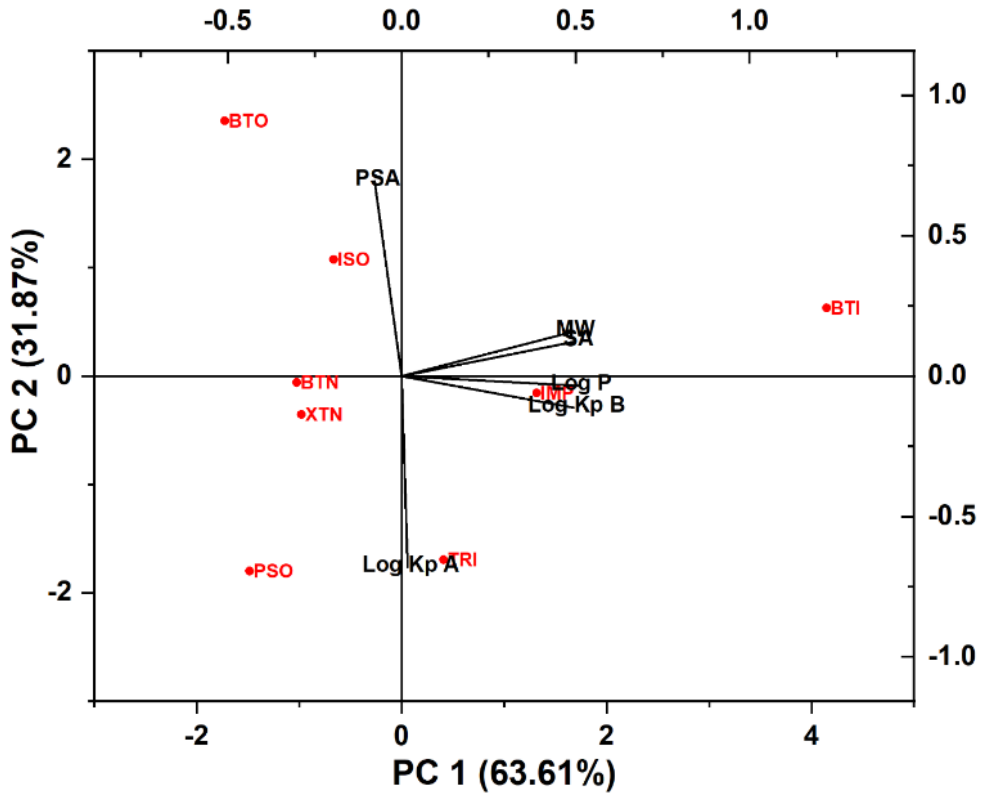


**Figure 1**

Notes: PCA biplot showcasing scatter plot of LF (red), eigenvector orientation and dimension according to the first two principal components (PC). MW stands for molecular weight; SA stands for the surface area; PSA stands for polar surface area, and Log $K_p$ stands for skin permeability coefficients gathered from different databases (A - pkCSM and B - SwissADME)

Results showcased that the first two principal components explain 95.48 % of the model's variance, suggesting that the results depicted herein are reproducible. Moreover, the first principal component explained 63.61 % of the model variance and promoted the separation of BTI from the other LF datasets, while the second principal component amassed 31.87 % of all variance (Figure 1). Furthermore, the eigenvectors representing molecular weight, surface area, Log $K_p$ B and Log P converged, which was further supported by the correlation matrix of the model. This suggests the positive influence of these factors towards better skin penetration. In addition, polar surface area and Log $K_p$ A eigenvectors showcased little convergence to the other descriptive vectors. However, their alignment suggests that their datasets may be inversely proportional, further supported in the correlation matrix (Figure 1).

The second step of this study involved the investigation of the predicted skin sensitization effects and toxicity of LF. Therefore, pkCSM and Pred-Skin databases were used, and the results are displayed in Table 3.

Table 3 – Predicted skin sensitization and toxicity of linear furanocoumarin derivatives, namely: BTI, BTN, BTO, IMP, ISO, PSO, TRI and XTN* (%)

| | SkinSenA** | SkinSenB*** | LLNA*** | DPRA*** | h-CLAT*** | KeratinoSens™ | Result*** |
|---|---|---|---|---|---|---|---|
| BTI | - | +80 | +60 | -60 | +60 | +80 | +60 |
| BTN | - | +80 | -50 | +60 | -50 | +80 | -50 |
| BTO | - | +80 | +70 | +70 | +70 | +80 | +60 |
| IMP | - | +80 | +60 | +60 | +60 | +90 | +60 |
| ISO | - | +70 | +50 | +60 | -50 | +80 | -60 |
| PSO | - | +80 | +60 | +60 | -50 | +100 | +50 |
| TRI | - | -50 | +50 | +70 | +60 | +60 | +80 |
| XTN | - | +80 | +60 | +60 | -50 | +100 | +50 |

Notes: *All data gathered at pkCSM and Pred-Skin databases upon imputing the SMILES string of each compound

**Categorical results at pkCSM. SkinSenA – skin sensitization pkCSM.

**Predicted results at Pred-Skin. SkinSenB – skin sensitization Pred-Skin; LLNA – murine local lymph node assay; DPRA – direct peptide reactivity assay; h-CLAT – human cell line activation test; Result – consensus model.

Results showcased that the pkCSM database suggested that no imputed LF would provide skin sensitization, while Pred-Skin suggested that most compounds promote this effect. Although Pred-Skin results are disclosed as categorical, a percentual score is given to support the reliability of the findings. In this sense, most LF was predicted as skin sensitizing agents with mode values of 80%. Moreover, Pred-Skin also provides predictive information about specific tests, namely LLNA; DPRA; h-CLAT and KeratinoSens®, as well as a consensus regarding the skin sensitization model. In this sense, most LF showcased positive results to the predicted data, albeit ranging from 50 to 60% in terms of statistical reliability. Notwithstanding, the consensus model for most LF was positive as skin sensitizer, even though BTN and ISO showcased adverse predicted outcomes (Table 3).

The third step of this investigation was the comparison of all LF chemical structures between themselves. Therefore, a pharmacophore model was rendered using PSO as a key-molecule. Results are depicted in Figure 2.

Results showcased that the core moiety furo [3,2-g] chromen-7-one was superimposed in the model (Figure 2.A), the distance between the nuclei of furan and central benzene moiety of 2.146 Å. In comparison, the distance between the nuclei of the central benzene and aromatic δ-valerolactone ring was 2.401 Å (Figure 2.B). The distances between the oxygens of the furan and aromatic δ-valerolactone ring were 4.781 Å, the distance between the oxygens in the carboxyl unit of this lactone 2.306 Å (Figure 2.C). In addition, the aromatic nuclei configuration presented an obtuse angle of 177.86º (Figure 2.D).

Considering that DNA intercalators such as ethidium bromide and acridine orange have similar tricyclic structures to LF, a pharmacophore model was rendered using these compounds and having PSO key-molecule. Results are depicted in figure 3.

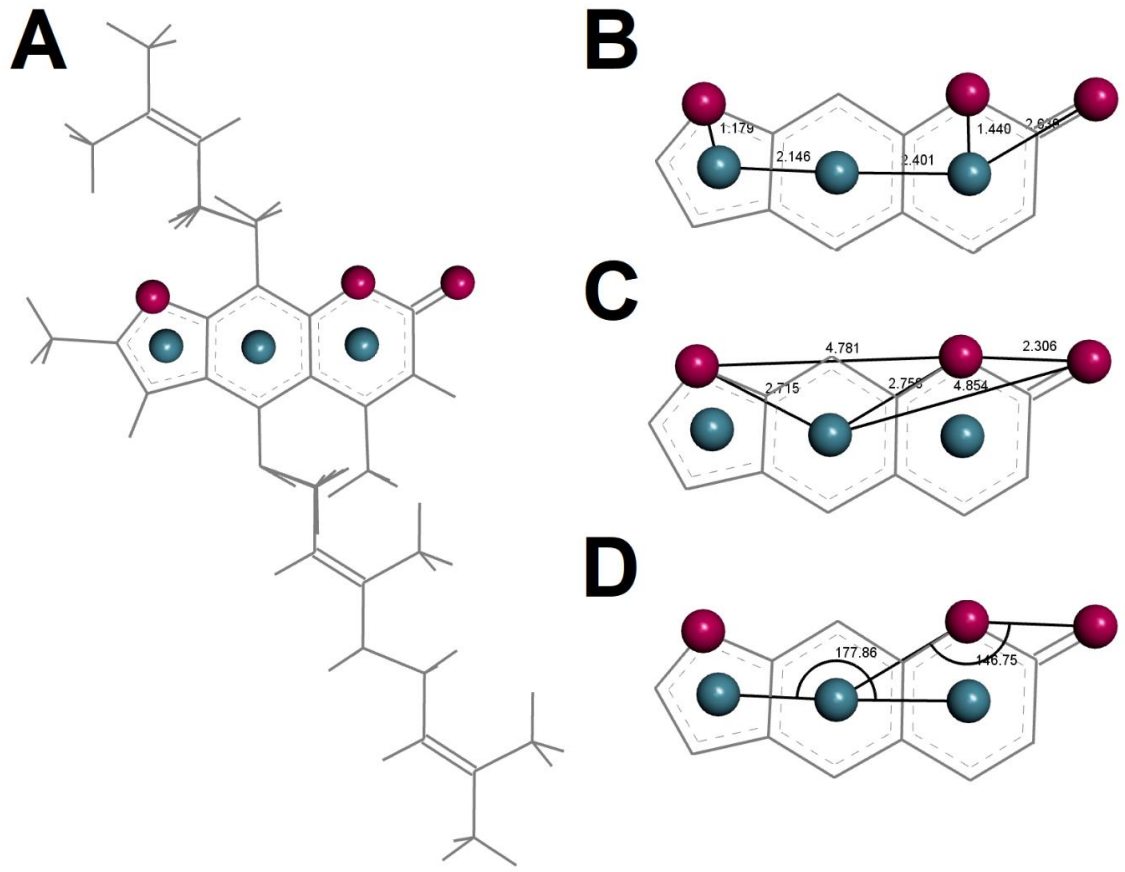


**Figure 2**

**Notes: A.** Pharmacophoric model of LF using BTI, BTN, BTO, IMP, ISO, PSO, TRI and XTN as inputs. **B, C and D.** Pharmacophoric model of linear furanocoumarins showcasing the distances (Å) and angles between the main contributors to the model. Red spheres represent the main contributors regarding hydrogen bond acceptors, while green spheres represent the main aromatic nuclei contributors

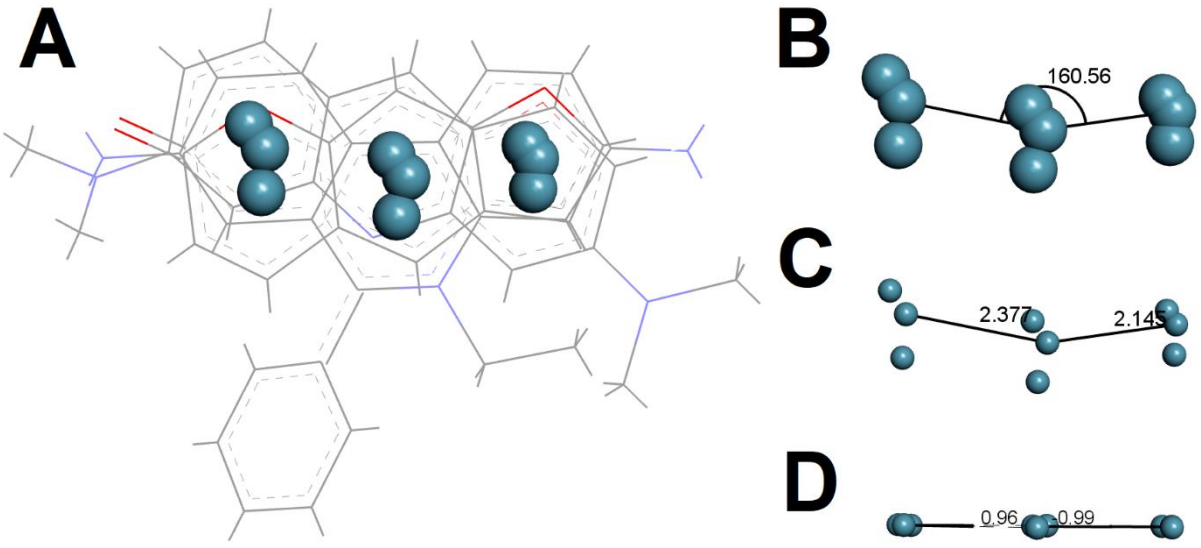


**Figure 3**

**Notes: A.** Pharmacophoric model using solely psoralen, acridine orange and ethidium bromide as inputs. **B, C and D.** Angles, distances and torsions between the aromatic contributors to the model. Green spheres represent the main aromatic nuclei contributors

Results showcased that the structures did not superimpose and, in the model, comprising only LF, an expected finding (Figure 3.A). The main model contributors were aromatic and positioned in three distinct points, whose angulation was 160.56º (Figure 3.B). Moreover, the external aromatic contributors showcased similar distances to the central one, about 2.261 Å (Figure 3.C). The contributors were almost planar, showcasing a negligible torsion (Figure 3.D).

Many authors discuss the photoreactivity of LF and its effects upon dermal administration [1, 2, 16]. Although the exact mechanisms underlying these effects are still unclear, literature attributes to the condensed aromatic system of Psoralens pro-oxidant properties [43, 44]. In this sense, some reports supported this interpretation due to the increased formation of reactive oxygen species in the presence of LF and similar compounds [19, 32, 44–46]. Notwithstanding, the furan ring of LF also features thermodynamic feasibility to covalently bind to several biologic receptors, which could explain both the therapeutic and toxic effects of these chemicals [9, 10, 47, 48].

In any case, most authors support that LF physicochemical features are of utmost importance to their effects, being structural characteristics like the condensed aromatic system often hinted as pharmacophores in both natural and synthetic components [29, 49–52], hence particular physicochemical and pharmacological attributes [53–55]. Moreover, this core moiety confers enough lipophilicity to these chemicals to allow their diffusion through the skin and cross other biological barriers such as the blood-brain barrier [56]. In this work, several databases provided similar physicochemical and pharmacokinetic information about LF (Table 1 and 2), being these data also supported by empiric research found in the literature [57–60]. Notwithstanding, the correlation of the findings through PCA showcased trends by other reports, such as the molecular weight, polar surface and Log P and Log $K_p$ B eigenvectors convergence (Figure 1). The correlation between these vectors suggests the relationship between structure weight and electron cloud when their lipophilicity and skin permeability are concerned. Nonetheless, many authors describe how similar compounds' chemical and electronic features may affect their pharmacokinetics *in silico* and *in vivo* investigations [57–59, 61, 62].

Considering the similar core structure shared by LF, the superimposition of their structures in the pharmacophore modelling was no surprise (Figure 2). The overall $sp^2$ hybridization of all carbons in the furo [3, 2-g] chromen-7-one moiety confers a planar orientation to the core of all LF [63]. This was nonetheless supported by energy minimization approaches based on "*Assisted Model Building with Energy Refinement*" toolkits [64], as well as *ab initio* investigations of similar compounds using density functional theory calculations [65]. In any case, LF core structure is regarded as a strong electron acceptor and donor, which supports their pro-oxidant behaviour and photoreactivity due to the possibility of electron transitions that may be involved in the biological effects of these compounds [13].

Previous reports evidenced that exposure to UV radiation is of upmost importance to the covalent binding of LF such as PSO to DNA bases, which further supports the involvement of the core moiety in the therapeutic or toxic effect of these chemicals [1, 66]. Moreover, when compared to well-known DNA intercalators ethidium bromide and acridine orange, the furo [3, 2-g] chromen-7-one moiety showcased similar aromatic contributors, as well as geometry, considering the planar orientation of these molecules (Figure 3). An important point must be addressed, though, which relies on the toxicodynamic of DNA intercalators such as the ones herein used for the pharmacophore modelling. Ethidium bromide and acridine orange link to DNA through covalent bonds and intermolecular interactions, being the kinetics and thermodynamics of this phenomenon subject of several investigations [12, 13]. PSO showcases similar behaviour regarding the involvement of both covalent bonds and intermolecular interactions. Considering the structural similarities herein discussed, the furo [3, 2-g] chromen-7-one moiety may be an essential contributor to dermal toxicity.

Regarding the predicted skin sensitization, pkCSM database results differed from the ones provided by Pred-Skin (Table 3). This difference may be attributed to distinct algorithms and weightings employed when imputed information was compiled [35,38,39]. Regardless of the case, Pred-Skin results were sound when compared to empiric investigations, which showcased the skin sensitizing effects of LF by different *in vitro* and *in vivo* approaches [1, 3, 59, 60]. Care must be taken, however, because these results imply by no means that one database is more reliable than

the other, considering the narrow scope of our investigation. Given the plethora of information found in all databases herein consulted, which was sound to empiric data, we suggest all the tools be used complementarily.

## CONCLUSIONS

This work investigated the predicted dermal toxicity of LF through chemoinformatic approaches. Results showcased that the molecular descriptor data can be used to predict the dermal toxicity of LF through *in silico* toolsets, which therefore shed light on the use of computational methods to predict the clinical outcomes of skin exposure to these compounds.

### Acknowledges

This study was financed in part by the Coordenação de Aperfeiçoamento de Pessoal de Nível Superior - Brasil (CAPES) - Finance Code 001.

### Conflict of interest

The authors declare that there is no conflict of interest.

## REFERENCES

1. Ibbotson, S. H. (2018). A Perspective on the Use of NB-UVB Phototherapy vs. PUVA Photochemotherapy. *Frontiers in medicine, 5*. doi: 10.3389/fmed.2018.00184
2. Stern, R. S. (2007). Psoralen and Ultraviolet A Light Therapy for Psoriasis. *New England Journal of Medicine, 357*(7), 682–690. doi: 10.1056/nejmct072317
3. Bethea, D., Fullmer, B., Syed, S., Seltzer, G., Tiano, J., Rischko, C., … Gasparro, F. P. (1999). Psoralen photobiology and photochemotherapy: 50 years of science and medicine. *Journal of Dermatological Science, 19*(2), 78–88. doi: 10.1016/s0923-1811(98)00064-4
4. Antunes, R. S., Thomaz, D. V., Garcia, L. F., Gil, E. de S., Sommerset, V. S., & Lopes, F. M. (2019). Determination of Methyldopa and Paracetamol in Pharmaceutical Samples by a Low Cost Genipa americana L. Polyphenol Oxidase Based Biosensor. *Advanced Pharmaceutical Bulletin, 9*(3), 416–422. doi: 10.15171/apb.2019.049
5. Da Cunha, C. E. P., Rodrigues, E. S. B., Fernandes Alecrim, M., Thomaz, D. V., Macêdo, I. Y. L., Garcia, L. F., … de Souza Gil, E. (2019). Voltammetric Evaluation of Diclofenac Tablets Samples through Carbon Black-Based Electrodes. *Pharmaceuticals, 12*(2), 83. doi: 10.3390/ph12020083
6. Garcia, L. F., da Cunha, C. E. P., Moreno, E. K. G., Vieira Thomaz, D., Lobón, G. S., Luque, R., … de Souza Gil, E. (2018). Nanostructured TiO2 Carbon Paste Based Sensor for Determination of Methyldopa. *Pharmaceuticals, 11*(4), 99. doi:10.3390/ph11040099
7. Garcia, L. F., da Cunha, C. E. P., Moreno, E. K. G., Vieira Thomaz, D., Lobón, G. S., Luque, R., … de Souza Gil, E. (2018). Nanostructured TiO2 Carbon Paste Based Sensor for Determination of Methyldopa. *Pharmaceuticals, 11*(4), 99. doi: 10.3390/ph11040099
8. Macêdo, I. Y. L. de, Alecrim, M. F., Oliveira Neto, J. R., Torres, I. M. S., Thomaz, D. V., & Gil, E. de S. (2020). Piroxicam voltammetric determination by ultra low cost pencil graphite electrode. *Brazilian Journal of Pharmaceutical Sciences, 56*. doi: 10.1590/s2175-97902019000317344
9. Alves, C. B., Rodrigues, E. S. B., Thomaz, D. V., Aguiar Filho, A. M. de, Gil, E. de S., & Couto, R. O. do. (2020). Correlation of polyphenol content and antioxidant capacity of selected teas and tisanes from Brazilian market. *Brazilian Journal of Food Technology, 23*. doi: 10.1590/1981-6723.03620
10. Contardi, U., Morikawa, M., & Thomaz, D. (2020). Redox Behavior of Central-Acting Opioid Tramadol and Its Possible Role in Oxidative Stress. *Medical Sciences Forum, 2*(1), 16. doi: 10.3390/cahd2020-08557
11. Cimino, G. D., Gamper, H. B., Isaacs, S. T., & Hearst, J. E. . (1985). Psoralens as photoactive probes of nucleic acid structure and function: organic chemistry, photochemistry, and biochemistry. *Annual Review of Biochemistry, 54*(1), 1151–1193. doi: 10.1146/annurev.bi.54.070185.005443

12. Da Silva, V. B., Kawano, D. F., Carvalho, I., Conceição, E. C., Freitas, O., & Silva, C. H. T. de P. (2009). Psoralen and Bergapten: In Silico Metabolism and Toxicophoric Analysis of Drugs Used to Treat Vitiligo. *Journal of Pharmacy & Pharmaceutical Sciences, 12*(3), 378. doi: 10.18433/j3w01d

13. Thomaz, D. V., de Oliveira, M. G., Rodrigues, E. S. B., da Silva, V. B., & dos Santos, P. A. (2020). Physicochemical Investigation of Psoralen Binding to Double Stranded DNA through Electroanalytical and Cheminformatic Approaches. *Pharmaceuticals, 13*(6), 108. doi: 10.3390/ph13060108

14. Nijsten, T. E. C., & Stern, R. S. (2003). The Increased Risk of Skin Cancer Is Persistent After Discontinuation of Psoralen+Ultraviolet A: A Cohort Study. *Journal of Investigative Dermatology, 121*(2), 252–258. doi: 10.1046/j.1523-1747.2003.12350.x

15. Oldham, M., Yoon, P., Fathi, Z., Beyer, W. F., Adamson, J., Liu, L., … Spector, N. L. (2016). X-Ray Psoralen Activated Cancer Therapy (X-PACT). *PLOS ONE, 11*(9), e0162078. doi: 10.1371/journal.pone.0162078

16. Menter, A., Gottlieb, A., Feldman, S. R., Van Voorhees, A. S., Leonardi, C. L., Gordon, K. B., … Bhushan, R. (2008). Guidelines of care for the management of psoriasis and psoriatic arthritis. *Journal of the American Academy of Dermatology, 58*(5), 826–850. doi: 10.1016/j.jaad.2008.02.039

17. Cardoso, C. A., Honda, N. K., & Barison, A. (2002). Simple and rapid determination of psoralens in topic solutions using liquid chromatography. *Journal of Pharmaceutical and Biomedical Analysis, 27*(1-2), 217–224. doi:10.1016/s0731-7085(01)00537-4

18. Diawara, M. M., Trumble, J. T., White, K. K., Carson, W. G., & Martinez, L. A. (1993). Toxicity of linear furanocoumarins toSpodoptera exigua: Evidence for antagonistic interactions. (11), 2473–2484. doi:10.1007/bf00980684

19. Schmitt, I. M., Chimenti, S., & Gasparro, F. P. (1995). Psoralen-protein photochemistry — a forgotten field. *Journal of Photochemistry and Photobiology B: Biology, 27*(2), 101–107. doi: 10.1016/1011-1344(94)07101-s

20. National Institute of Environmental Health Sciences. (1999). *The Murine Local Lymph Node Assay. A Test Method for Assessing the Allergic Contact Dermatitis Potential of Chemicals/Compounds*. Retrieved from https://ntp.niehs.nih.gov/iccvam/docs/immunotox_docs/llna/llnarep.pdf

21. Lalko, J. F., Kimber, I., Gerberick, G. F., Foertsch, L. M., Api, A. M., & Dearman, R. J. (2012). The Direct Peptide Reactivity Assay: Selectivity of Chemical Respiratory Allergens. *Toxicological Sciences, 129*(2), 421–431. doi: 10.1093/toxsci/kfs205

22. Nukada, Y., Ashikaga, T., Miyazawa, M., Hirota, M., Sakaguchi, H., Sasa, H., & Nishiyama, N. (2012). Prediction of skin sensitization potency of chemicals by human Cell Line Activation Test (h-CLAT) and an attempt at classifying skin sensitization potency. *Toxicology in Vitro, 26*(7), 1150–1160. doi: 10.1016/j.tiv.2012.07.001

23. Emter, R., van der Veen, J. W., Adamson, G., Ezendam, J., van Loveren, H., & Natsch, A. (2013). Gene expression changes induced by skin sensitizers in the KeratinoSens™ cell line: Discriminating Nrf2-dependent and Nrf2-independent events. *Toxicology in Vitro, 27*(8), 2225–2232. doi: 10.1016/j.tiv.2013.09.009

24. Flaten, G. E., Palac, Z., Engesland, A., Filipović-Grčić, J., Vanić, Ž., & Škalko-Basnet, N. (2015). In vitro skin models as a tool in optimization of drug formulation. *European Journal of Pharmaceutical Sciences, 75*, 10–24. doi: 10.1016/j.ejps.2015.02.018

25. Xu, J., & Hagler, A. (2002). Chemoinformatics and Drug Discovery. *Molecules, 7*(8), 566–600. doi: 10.3390/70800566

26. Wegner, J. K., Sterling, A., Guha, R., Bender, A., Faulon, J.-L., Hastings, J., … Willighagen, E. (2012). Cheminformatics. *Communications of the ACM, 55*(11), 65–75. doi: 10.1145/2366316.2366334

27. In silico investigation of possible caffeine interactions with common inflammation-related targets. (2019). *Journal of Applied Biology & Biotechnology, 7*(5), 31–34. doi: 10.7324/jabb.2019.70505

28. Thomaz, D. V., Rodrigues, E. S. B., & de Macedo, I. Y. L. (2019). Chemoinformatic Approaches in the Study of Fluralaner and Afoxolaner-mediated Inhibition of l-glutamate-gated Chloride Channels. *Path of Science, 5*(3), 4001–4007. doi: 10.22178/pos.44-6

29. Cherkasov, A., Muratov, E. N., Fourches, D., Varnek, A., Baskin, I. I., Cronin, M., … Tropsha, A. (2014). QSAR Modeling: Where Have You Been? Where Are You Going To? *Journal of Medicinal Chemistry, 57*(12), 4977–5010. doi: 10.1021/jm4004285

30. Yang, S.-Y. (2010). Pharmacophore modeling and applications in drug discovery: challenges and recent advances. *Drug Discovery Today, 15*(11-12), 444–450. doi: 10.1016/j.drudis.2010.03.013

31. Lino, R. C., da Silva, D. P. B., Florentino, I. F., da Silva, D. M., Martins, J. L. R., Batista, D. da C., … Costa, E. A. (2017). Pharmacological evaluation and molecular docking of new di-tert-butylphenol compound, LQFM-091, a new dual 5-LOX/COX inhibitor. *European Journal of Pharmaceutical Sciences, 106*, 231–243. doi: 10.1016/j.ejps.2017.06.006

32. Thomaz, D. V., Rodrigues, E. S. B., Machado, F. B., … Macedo, I. Y. L. (2019). Investigation of Cyclobenzaprine Interactions with P450 Cytochromes CYP1A2 and CYP3A4 through Molecular Docking Tools. *Path of Science, 5*(2), 4001–4006. doi: 10.22178/pos.43-1

33. Weininger, D. (1988). SMILES, a chemical language and information system. 1. Introduction to methodology and encoding rules. *Journal of Chemical Information and Modeling, 28*(1), 31–36. doi: 10.1021/ci00057a005

34. Rajanarendar, E., Rama Krishna, S., Nagaraju, D., Govardhan Reddy, K., Kishore, B., & Reddy, Y. N. (2015). Environmentally benign synthesis, molecular properties prediction and anti-inflammatory activity of novel isoxazolo[5,4-d]isoxazol-3-yl-aryl-methanones via vinylogous Henry nitroaldol adducts as synthons. *Bioorganic & Medicinal Chemistry Letters, 25*(7), 1630–1634. doi: 10.1016/j.bmcl.2015.01.041

35. Pires, D. E. V., Blundell, T. L., & Ascher, D. B. (2015). pkCSM: Predicting Small-Molecule Pharmacokinetic and Toxicity Properties Using Graph-Based Signatures. *Journal of Medicinal Chemistry, 58*(9), 4066–4072. doi: 10.1021/acs.jmedchem.5b00104

36. Daina, A., & Zoete, V. (2019). Application of the SwissDrugDesign Online Resources in Virtual Screening. *International Journal of Molecular Sciences, 20*(18), 4612. doi:10.3390/ijms20184612

37. Daina, A., Michielin, O., & Zoete, V. (2017). SwissADME: a free web tool to evaluate pharmacokinetics, drug-likeness and medicinal chemistry friendliness of small molecules. *Scientific Reports, 7*(1). doi: 10.1038/srep42717

38. Braga, R. C., Alves, V. M., Muratov, E. N., Strickland, J., Kleinstreuer, N., Trospsha, A., & Andrade, C. H. (2017). Pred-Skin: A Fast and Reliable Web Application to Assess Skin Sensitization Effect of Chemicals. *Journal of Chemical Information and Modeling, 57*(5), 1013–1017. doi: 10.1021/acs.jcim.7b00194

39. Golden, E. (2020). Evaluation of the global performance of eight in silico skin sensitization models using human data. *ALTEX*. doi: 10.14573/altex.1911261

40. Dror, O., Schneidman-Duhovny, D., Inbar, Y., Nussinov, R., & Wolfson, H. J. (2009). Novel Approach for Efficient Pharmacophore-Based Virtual Screening: Method and Applications. *Journal of Chemical Information and Modeling, 49*(10), 2333–2343. doi: 10.1021/ci900263d

41. Schneidman-Duhovny, D., Dror, O., Inbar, Y., Nussinov, R., & Wolfson, H. J. (2008). PharmaGist: a webserver for ligand-based pharmacophore detection. *Nucleic Acids Research, 36*(Web Server), W223–W228. doi: 10.1093/nar/gkn187

42. Syms, C. (2008). Principal Components Analysis. *Encyclopedia of Ecology*, 2940–2949. doi: 10.1016/b978-008045405-4.00538-3

43. Deng, M., Xie, L., Zhong, L., Liao, Y., Liu, L., & Li, X. (2020). Imperatorin: A review of its pharmacology, toxicity and pharmacokinetics. *European Journal of Pharmacology, 879*, 173124. doi: 10.1016/j.ejphar.2020.173124

44. Aboul-Enein, H. Y., Kladna, A., Kruk, I., Lichszteld, K., & Michalska, T. (2002). Effect of psoralens on Fenton-like reaction generating reactive oxygen species. *Biopolymers, 72*(1), 59–68. doi: 10.1002/bip.10285

45. Fröbel, S., Reiffers, A., Torres Ziegenbein, C., & Gilch, P. (2015). DNA Intercalated Psoralen Undergoes Efficient Photoinduced Electron Transfer. *The Journal of Physical Chemistry Letters, 6*(7), 1260–1264. doi: 10.1021/acs.jpclett.5b00307

46. Kussmaul Gonçalves Moreno, E. (2019). Antioxidant Study and Electroanalytical Investigation of Selected Herbal Samples Used in Folk Medicine. *International Journal of Electrochemical Science*, 838–847. doi: 10.20964/2019.01.82

47. Thomaz, D. V., Peixoto, L. F., de Oliveira, T. S., Fajemiroye, J. O., da Silva Neri, H. F., Xavier, C. H., … Ghedini, P. C. (2018). Antioxidant and Neuroprotective Properties of Eugenia dysenterica Leaves. *Oxidative Medicine and Cellular Longevity, 2018*, 1–9. doi: 10.1155/2018/3250908

48. Vieira Thomaz, D. (2018). Assessment of Noni (Morinda citrifolia L.) Product Authenticity by Solid State Voltammetry. *International Journal of Electrochemical Science*, 8983–8994. doi: 10.20964/2018.09.390

49. Marzaro, G., Guiotto, A., Borgatti, M., Finotti, A., Gambari, R., Breveglieri, G., & Chilin, A. (2013). Psoralen Derivatives as Inhibitors of NF-κB/DNA Interaction: Synthesis, Molecular Modeling, 3D-QSAR, and Biological Evaluation. *Journal of Medicinal Chemistry, 56*(5), 1830–1842. doi: 10.1021/jm3009647

50. Giordanetto, F., Fossa, P., Menozzi, G., & Mosti, L. (2003). In silico rationalization of the structural and physicochemical requirements for photobiological activity in angelicine derivatives and their heteroanalogues. *Journal of computer-aided molecular design, 17*(1), 53–64. doi: 10.1023/a:1024557113083

51. Gia, O., Marciani Magno, S., Gonzalez-Diaz, H., Quezada, E., Santana, L., Uriarte, E., & Dalla Via, L. (2005). Design, synthesis and photobiological properties of 3,4-cyclopentenepsoralens. *Bioorganic & Medicinal Chemistry, 13*(3), 809–817. doi: 10.1016/j.bmc.2004.10.044

52. Vieira Thomaz, D. (2021). Thermodynamics and Kinetics of Camellia sinensis Extracts and Constituents: An Untamed Antioxidant Potential. *Bioactive Compounds in Nutraceutical and Functional Food for Good Human Health*. doi: 10.5772/intechopen.92813

53. Leite, K. C. de S., Garcia, L. F., Lobón, G. S., Thomaz, D. V., Moreno, E. K. G., Carvalho, M. F. de, … Gil, E. de S. (2018). Antioxidant activity evaluation of dried herbal extracts: an electroanalytical approach. *Revista Brasileira de Farmacognosia, 28*(3), 325–332. doi: 10.1016/j.bjp.2018.04.004

54. Chaibub, B. A., Parente, L. M. L., Lino Jr, R. de S., Cirilo, H. N. C., Garcia, S. A. de S., Nogueira, J. C. M., … Bara, M. T. F. (2020). Investigation of wound healing activity of Lafoensia pacari (Lythraceae) leaves extract cultivated in Goiás state, Brazil. *Rodriguésia, 71*. doi: 10.1590/2175-7860202071058

55. Lima Morais, R., Ferreira Garcia, L., Kussmaul Gonçalves Moreno, E., Vieira Thomaz, D., De Brito Rodrigues, L., Barroso Brito, L., … Gil, E. D. S. (2019). Electrochemical remediation of industrial pharmaceutical wastewater containing hormones in a pilot scale treatment system. *Eclética Química Journal, 44*(1), 40. doi: 10.26850/1678-4618eqj.v44.1.2019.p40-52

56. Mensch, J., Melis, A., Mackie, C., Verreck, G., Brewster, M. E., & Augustijns, P. (2010). Evaluation of various PAMPA models to identify the most discriminating method for the prediction of BBB permeability. *European Journal of Pharmaceutics and Biopharmaceutics, 74*(3), 495–502. doi: 10.1016/j.ejpb.2010.01.003

57. Li, Y., Duan, J., Guo, T., Xie, W., Yan, S., Li, B., … Chen, Y. (2009). In vivo pharmacokinetics comparisons of icariin, emodin and psoralen from Gan-kang granules and extracts of Herba Epimedii, Nepal dock root, Ficus hirta yahl. *Journal of Ethnopharmacology, 124*(3), 522–529. doi: 10.1016/j.jep.2009.05.008

58. Wang, Y.-F., Liu, Y.-N., Xiong, W., Yan, D.-M., Zhu, Y., Gao, X.-M., … Qi, A.-D. (2014). A UPLC–MS/MS method for in vivo and in vitro pharmacokinetic studies of psoralenoside, isopsoralenoside, psoralen and isopsoralen from Psoralea corylifolia extract. *Journal of Ethnopharmacology, 151*(1), 609–617. doi: 10.1016/j.jep.2013.11.013

59. De Wolff, F. A., & Thomas, T. V. (1986). Clinical Pharmacokinetics of Methoxsalen and Other Psoralens. *Clinical Pharmacokinetics, 11*(1), 62–75. doi: 10.2165/00003088-198611010-00004

60. Martins, F. S., Sy, S. K. B., Fonseca, M. J. V., & de Freitas, O. (2020). Pharmacokinetics, Pharmacodynamics and Dermal Distribution of 5-Methoxypsoralen Based on a Physiologically Based Pharmacokinetic Model to Support Phytotherapy Using Brosimum gaudichaudii. *Planta Medica, 86*(04), 276–283. doi: 10.1055/a-1087-8374

61. Wagner, J. G. (1988). *Pharmacokinetic Studies in Man*. Retrieved from https://www.ema.europa.eu/en/documents/scientific-guideline/pharmacokinetic-studies-man_en.pdf

62. Kenny, P. W. (2009). Hydrogen Bonding, Electrostatic Potential, and Molecular Design. Journal of *Chemical Information and Modeling, 49*(5), 1234–1244. doi: 10.1021/ci9000234

63. Ouellette, R. J., & Rawn, J. D. (2014). *Organic Chemistry. Structure, Mechanism, and Synthesis*. doi: 10.1016/c2013-0-14256-0

64. Pearlman, D. A., Case, D. A., Caldwell, J. W., Ross, W. S., Cheatham, T. E., DeBolt, S., … Kollman, P. (1995). AMBER, a package of computer programs for applying molecular mechanics, normal mode analysis, molecular dynamics and free energy calculations to simulate the structural and energetic properties of molecules. *Computer Physics Communications, 91*(1-3), 1–41. doi: 10.1016/0010-4655(95)00041-d

65. Rodrigues, E. S. B., de Macêdo, I. Y. L., da Silva Lima, L. L., Thomaz, D. V., da Cunha, C. E. P., Teles de Oliveira, M., … de Souza Gil, E. (2019). Electrochemical Characterization of Central Action Tricyclic Drugs by Voltammetric Techniques and Density Functional Theory Calculations. *Pharmaceuticals, 12*(3), 116. doi: 10.3390/ph12030116

66. Thomaz, D., & Santos, P. (2021). Electrochemical behavior of Methotrexate upon binding to the DNA of different cell lines. *Proceedings of The 1st International Electronic Conference on Cancers: Exploiting Cancer Vulnerability by Targeting the DNA Damage Response*. doi: 10.3390/iecc2021-09215